Experimental Investigation about the Mechanism of Fission-Fragment Induced Desorption*

N. Fürstenau, W. Knippelberg, F. R. Krueger, G. Weiß, and K. Wien

Institut für Kernphysik der Technischen Hochschule Darmstadt

(Z. Naturforsch. **32 a**, 711–719 [1977]; received June 14, 1977)

The physical processes involved in the fission-fragment induced desorption of molecular and atomic ions from surfaces have been investigated by measuring absolute ion yields, distributions of radial and axial initial energy components and isotopic effects. For this purpose several modifications of the time-of-flight spectrometer were put in practice. By studying multiple ion desorption per fission-fragment correlations between various molecular fragments were identified. The results are compared with predictions of reaction models. The observed phenomena are in agreement with a break-down of the polar-binding potential at the surface caused partially by the low energy electron plasma produced by the fission-fragment.

1. Introduction

Since the first communication of Macfarlane and coworkers [1] about the fission-fragment induced desorption and its application to mass-spectroscopy, numerous spectra of mostly organic compounds have been measured, but only little is known about the desorption process itself. A better understanding of these processes would be important for the physics of ion energy loss in matter but also clarify the field of applications and its limits.

Considering the main features of the mass spectra [2] the fragmentation of the molecules by the desorption process is remarkably poor compared to the enormous energy deposit of the fragments in the target. Their pattern is similar to those of field-desorption spectra measured at high target temperatures. In addition to fragments also undestroyed molecular ions are observed, protonated in the case of positive and deprotonated in the case of negative ions. As confirmed by McNeal and Macfarlane for the amino acid Valine [3] the last phenomenon is due to proton transfer reactions, a typical ionization process for organic molecules at moderate excitation energies.

In order to study the desorption mechanism we inquired in detail the properties of the desorbed ions such as their initial energy and angular distribution. Also absolute yields of desorbed ions per fission fragment and isotopic effects were investigated. For all these measurements the time-of-flight technique has been applied, which allows also the registration of multiple ion-desorption per fragment. The latter gives information about correlations between molecular fragments. As discussed in this paper our results do not agree with a thermal spike hypothesis presented by Macfarlane and Torgerson [4]. We seem to be able to explain our data in terms of a "dynamic field desorption" caused by the strong, short-lived electronic plasma, which is produced by the fast heavy fission-fragment traversing the target.

* Supported by the Deutsche Forschungsgemeinschaft (DFG).

Reprint requests to Prof. Dr. K. Wien, Institut für Kernphysik der Technischen Hochschule Darmstadt, Schloßgartenstraße 9, *D-6100 Darmstadt*.

2. Experimental Methods

2.1. Principle of Operation

Till now the fission-fragment induced desorption has been studied only by a time-of-flight technique described elsewhere [5–7]. The target, a thin layer of the sample on a metallic foil, is bombarded by the fast fragments of a ^{252}Cf fission source. The desorbed ions emerging from the surface of the target are accelerated by an homogeneous electric field. Their time of flight after passing a certain distance is measured by electronic means as time period between the arrival of the fission-fragment in a detector closely behind the target foil and a signal in an iondetector at the end of the flight path. As long as the acceleration voltage is much higher than the initial energy of the desorbed ions, the time spectrum shows a pronounced line for each ion mass. The time-of-flight is proportional to the square root of the mass, its spectrum is recorded, for instance, by a multichannel-analyzer.

2.2. Recent Improvements of the Apparatus

In order to have a more radiation resistant start detector, the semiconductor detector used so far [7] was replaced by the detector shown in Figure 1.

The fast fission-fragments traversing the 0.5 μm thick "converter" foil cause the emission of secondary electrons being accelerated onto a channel-plate

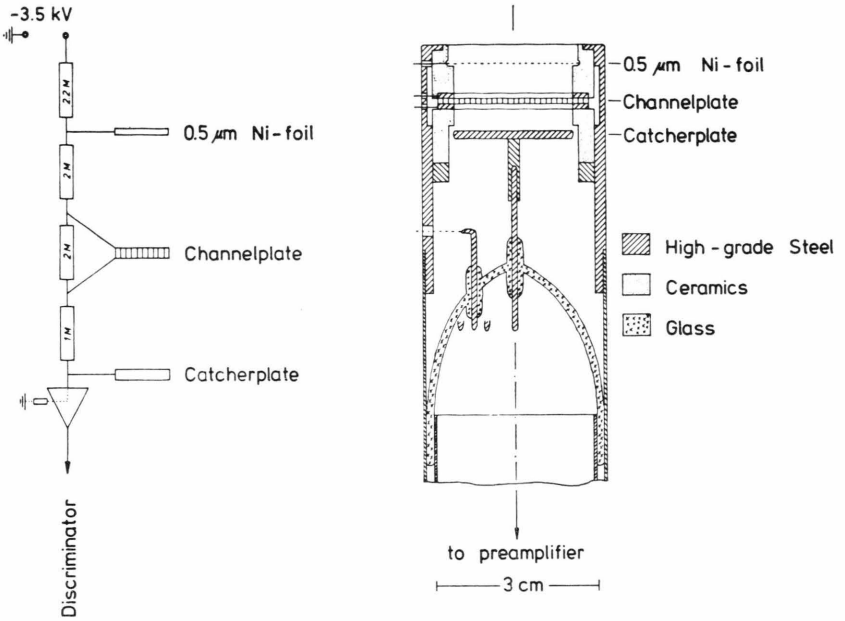

Fig. 1. Start-detector of the time-of-flight spectrometer. Mechanical arrangement and voltage-divider.

(Valvo G25). After an amplification by a factor of about 10^3 the electrons behind the channel-plate are collected on a catcher-plate closely connected to a fast, voltage sensitive preamplifier *. The output pulses have rise times of typically 1 nsec. The α-particles of the ^{252}Cf source produce smaller signals than the fission-fragments and can be suppressed by pulse-height discrimination in the succeeding constant fraction discriminator [7]. The new detector is bakable up to 300 °C.

With this detector the electronic part of the time resolution is below 1 nsec, but the observed line width was never smaller than 1.5 nsec – even at acceleration voltages $U_a > 10$ kV. Figure 2 shows the mass line of H^+ measured at $U_a = 17$ kV. The reason for the double peaked line shape is the natural velocity distribution of the fission-fragments. After their impact in the target, which is the actual start point of the time of flight, they have to pass a distance of 2 cm before hitting the start detector. The lighter group of fission-fragments has higher velocities than the heavier group and produces therefore earlier start signals. In order to avoid this effect, a detector is under construction, which collects the secondary electrons directly from the backside of the target foil.

With the flight path of 120 cm the optimum mass resolution obtained was 900 for $U_a = 11$ kV. At this flight path a certain part of the phase space volume of the desorbed ions is not accepted by the apparatus, – especially for ions with high initial radial velocities. All measurements for chemical purpose were performed by this medium resolution arrangement.

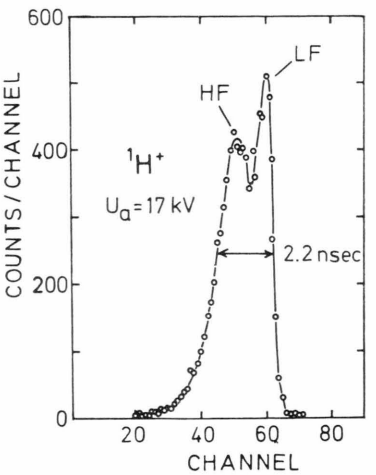

Fig. 2. Mass-line of $^1H^+$-ions measured with $U_a \gg E_y$. HF: Part of the line caused by the heavy group of fission fragments, LF: Part of the line caused by the light group.

2.3. Low Resolution System of High Acceptance

In order to measure the density of the phase space of the desorbed ions and their absolute yields, the flight path has been reduced to 13.6 cm and 22.6 cm, respectively. Above a certain value of U_a all ions are now accepted by the active area ($\Phi =$

* The preamplifier has been developed by J. Foh, Institut für Kernphysik der Technischen Hochschule Darmstadt.

4 cm) of the stop detector. The mass resolution, however, has become considerably lower, that means, the investigated lines have to be well isolated from neighbouring lines.

2.3.1. Measurement of $\Delta N/\Delta E_r$

As illustrated in Fig. 3 the chance for an desorbed ion to hit the stop detector depends on its initial radial velocity v_r, the acceleration voltage U_a and the diameter Φ_s of the iris mounted in front of the stop detector. Therefore, the distribution of v_r can be determined by two independent methods, either by measuring the intensity of the regarded mass line as function of U_a with $\Phi_s = \text{const}$ or vice versa as function of Φ_s with $U_a = \text{const}$. Going from one U_a- or Φ_s-value to the next one reduces or extends the acceptance for another v_r interval. Differentiation of the measured curves delivers the desired distribution $\Delta N/\Delta v_r$, which can be transformed into a radial energy distribution $\Delta N/\Delta E_r$. The v_r- or E_r-scale was evaluated from the corresponding time-of-flight values and iris diameters.

2.3.2. Measurement of $\Delta N/\Delta E_z$

At full acceptance the line shape delivers almost directly the distribution of the axial component v_z of the initial velocity, if the line width is significantly larger than the time resolution of the apparatus. This is generally the case at U_a values of 300 Volt or below. To detect these low energetic ions an additional potential of 2.8 kV was applied between the front plate of the stop detector and a grid in front of it.

A more serious problem is the determination of that point of the time scale, which corresponds to $v_z = 0$ for a certain mass line. For this purpose firstly the absolute zero point of the time scale was determined by measuring the time of flight of secondary electrons produced by the fission fragment in the target. They traverse the flight path in only a few nsec at $U_a = 10$ kV for instance.

Secondly the time of flight for the regarded ion mass was accurately calculated using the precisely measured distances of the flight path and acceleration voltages. In this calculation a final adjustment to the drift part of the flight path was done with help of mass lines measured at high acceleration voltages, where the influence of v_z to the line shape is negligible. With the known $v_z = 0$ point it was no problem to replace the time scale under a mass line by a corresponding velocity or energy scale and to evaluate $\Delta N/\Delta E_z$. The position of the different scales is illustrated in Figure 4.

2.3.3. Measurement of Multiple Ion Desorption per Fission-Fragment

Measuring absolute yields of desorbed ions one has to consider the possibility that more than one ion per fragment emerges from the target. Because the time-to-amplitude converter of the electronic system [7] is able to record only the first ion within its active time period, lighter ions are detected with greater probability than heavier ones. True yields for certain ions can be obtained by help of coincidence methods as described in Reference [7]. A more simple method is to suppress the preceding part of

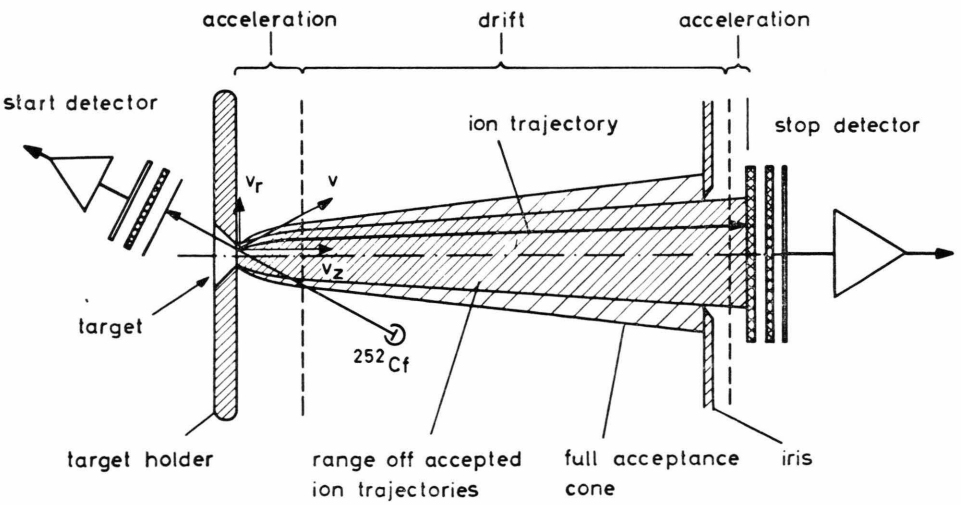

Fig. 3. Schematic diagramme of the time-of-flight system showing the range of ion-trajectories for limited and full acceptance. v, v_r and v_z are the initial velocity and velocity components of the desorbed ions.

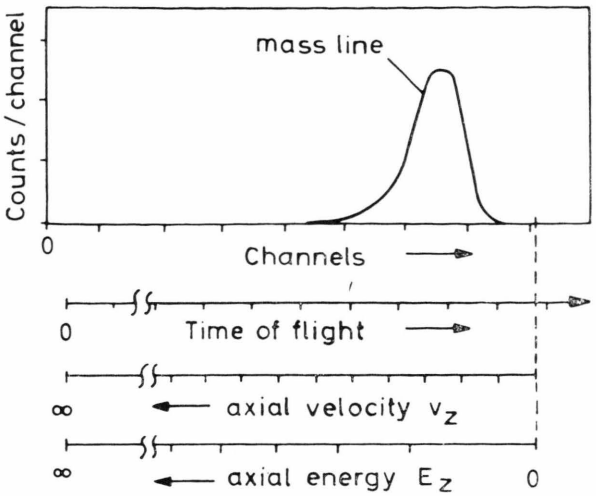

Fig. 4. Illustration about the determination of the axial energy distribution (see text).

the spectrum till the regarded mass line using a delay-generator behind the start-detector. The first line of the spectrum is then always observed with its true intensity. The appearance of several ions per fragment can be purely statistical or correlated as seen in Chapter 3.4.

It is not in the scope of this paper to describe the mathematical methods used for the evaluation of initial energy distributions and correlations [8].

3. Experimental Results

The following experiments have been carried out with LiCl, CsBr, Atropine and Thiamine targets being electrosprayed [7, 9] onto a 5 μm-Al foil. The target layer had a thickness of typically 100 ng/cm^2, its effective diameter was 6 mm. The measurements, however, were analyzed assuming a point target. Monte Carlo calculations proved that the 6 mm diameter has only little influence on the evaluated energy distributions. All targets were irradiated from the front side. Only positively charged ions were studied, but as shown by Macfarlane and coworkers [10] negative ions have a similar behaviour.

3.1. The Radial Energy Distribution

This distribution was treated by both methods mentioned in Chapter 2.3.1. The first method requires a change of U_a causing problems with the detection efficiency. Therefore, more reliable results were obtained with a second method. Figure 5 shows the intensity of the Atropine ion M^+ as function of

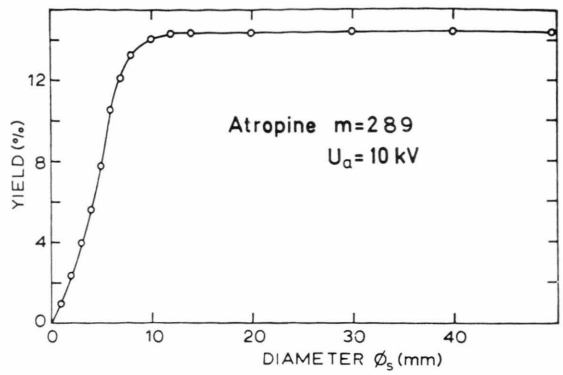

Fig. 5. Yield of the Atropine M^+ ions as function of the iris diameter measured with a flight path of 13.6 cm.

the iris diameter Φ_s at $U_a = 10$ kV. Above $\Phi_s =$ 13 mm full acceptance is achieved. Transforming the Φ_s-values into radial energy values and differentiation of the curve in Fig. 5 gives the $\Delta N/\Delta E_r$ distri-

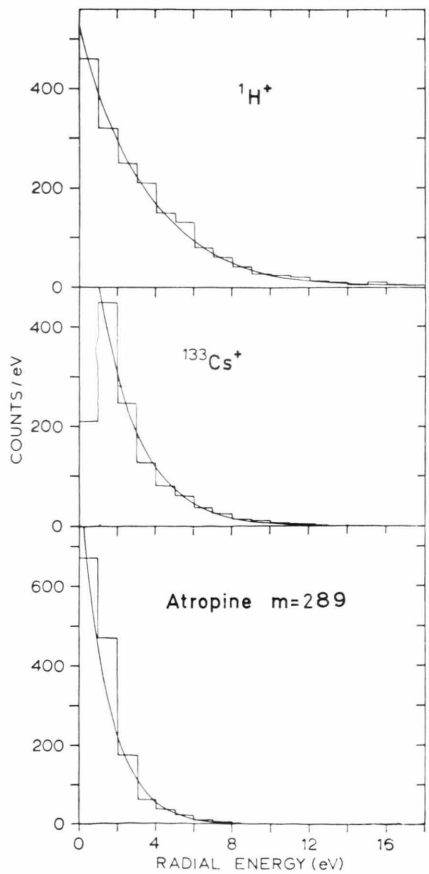

Fig. 6. Radial energy distribution of $^1H^+$ (6 a), ^{133}Cs (6 b) and Atropine M^+ ions (6 c). The solid lines represent functions calculated with the parameters of Table 1.

Table 1.

Ion	λ_r (eV^{-1})	Yield (%)
$^1H^+$	0.29 ± 0.05	33 ± 7
$^{133}Cs^+$	0.48 ± 0.07	11 ± 2
$(Atropine)^+$	0.70 ± 0.07	26 ± 5

bution in Figure 6 c. Similar measurements were performed for the $^1H^+$ and $^{133}Cs^+$ ions (Fig. 6 a and 6 b).

All measured radial energy distributions are peaked near or at $E_r = 0$ with an exponential decrease to higher E_r-values. They are given by

$$\Delta N/\Delta E_r = A_r \cdot \exp\{-\lambda_r E_r\}.$$

The values λ_r and the saturation yields per fission fragment are given in Table 1. The latter are corrected for transmission and detection efficiency handled in Chapter 3.3.

The values λ_r have to be considered with caution because the surface of the target has certainly not an even microstructure. That means, the perpendicular of the surface microelements does not or rarely coincide with the spectrometer axis. Therefore, a phase space mixing takes place and higher energetic axial components may contribute to the observed radial energy distribution causing a shift to lower values of λ_r.

3.2. The Axial Energy Distribution

With decreasing acceleration voltage the axial component of the initial ion energy becomes finally the dominant quantity for the line shape. At $U_a = 300$ V the time resolution of the apparatus is generally 2 or 3 times smaller than the line width. In Fig. 7 the mass line of $^{133}Cs^+$ ions is presented measured with a flight path of 13.6 cm. The time scale was converted into an energy scale by the procedure described in Chapter 2.3.2.

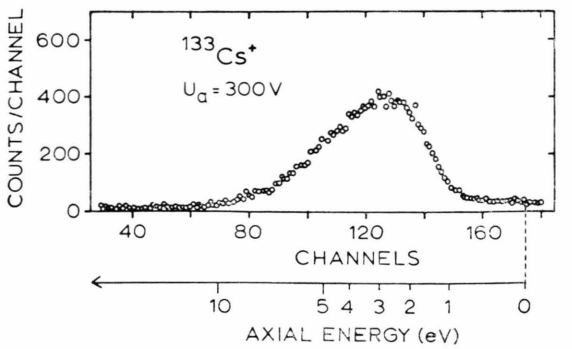

Fig. 7. Mass line of $^{133}Cs^+$ ions measured at $U_a = 300$ V.

The corresponding axial energy distribution is shown in Fig. 8 together with two other examples obtained for $^1H^+$ and $^7Li^+$ ions. Distributions for organic molecule ions will be taken with a stronger ^{252}Cf source in the near future.

The presented distributions are not of Maxwell type, which would be almost an exponential function. They can be fitted well by

$$\Delta N/\Delta E_z = A_z (E_z - E_0)^a \cdot \exp\{-\lambda_z (E_z - E_0)\} \qquad E_z > E_0$$

Table 2.

Ion	E_0 (eV)	a	λ_z (eV^{-1})	$\overline{E}_z$ (eV)
$^1H^+$	0.0	2.0 ± 0.3	0.3 ± 0.1	9.7
$^7Li^+$	0.0	3.7 ± 0.5	1.7 ± 0.7	2.6
$^{133}Cs^+$	0.6	1.5 ± 0.3	0.8 ± 0.3	3.5

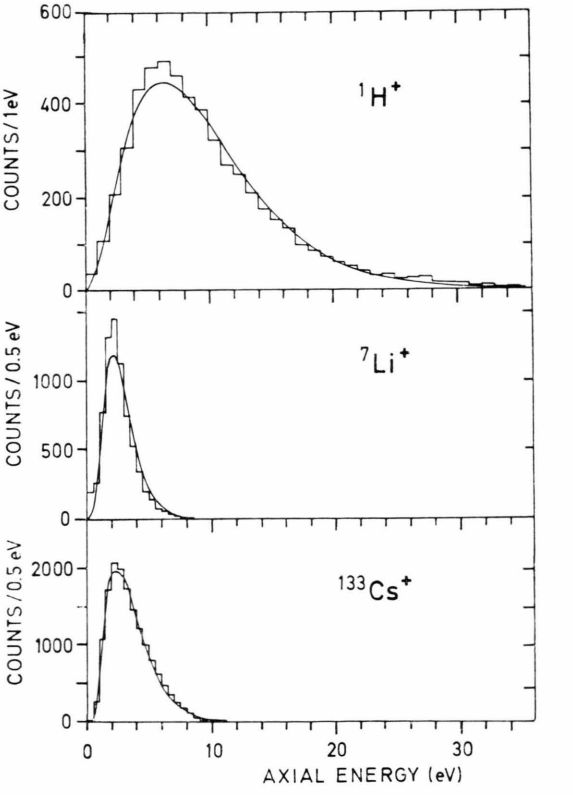

Fig. 8. Axial energy distributions of $^1H^+$, $^7Li^+$ and $^{133}Cs^+$ ions measured at $U_a = 300$ V. The solid lines represent functions calculated with the parameters of Table 2.

The observed parameters E_0, a and λ_z are given in Table 2. E_0 can be interpreted as a minimum of activation energy the ion needs to overcome the surface potential field. Also in this case the microstructure of the surface causes a mixing of the phase space and may, therefore, add low energy events to the measured distributions. On the other side till now the experimental accuracy of determing E_0 is not sufficient to decide whether $E_0 = 0$ or not. The uncertainties of the measurements are bigger than typical chemical activation energies. However, charged induced desorption could give measurable E_0 values.

3.3. Yields of Desorbed Ions

Yields were always related to the number of fission fragments received by the start detector. The time of flight events measured at full acceptance had to be corrected for the transmission of the grids (0.77) and the detection efficiency of the stop detector, i. e. of the channel plate. The latter, a rather inaccurately known figure, was taken from literature as 0.7 ± 0.2 for 10 keV ions [11].

The determination of total ion yields carried out by methods mentioned in Chapter 2.3.3 is rather circumstantial. If the ions are desorbed independently from the surface, the probability for the emission of a certain number of ions per fission fragment should be Poisson distributed. With this assumption the mean yield per fragment can be calculated using the total number of observed events and the number of start events without ion desorption. This procedure was applied to the mass spectrum of Thiamine. The mean total yield per fission fragment was found to be

$$\overline{S}_{\text{total}} = 2.4 \pm 0.6 .$$

Here background events have not been subtracted. Actually it is often impossible to decide whether a certain mass line is a background line or not. Especially Na^+ and K^+ ions produced generally intensive background lines. Table 1 presents the yields of $^1H^+$, $^{133}Cs^+$ and Atropine M^+ ions. The yield of a certain line never exceeds 40%. The total negative ion currents are somewhat smaller than the positive ones. The cross section for desorption was estimated to be about 10^{-15} cm^2.

An isotopic effect was observed for the desorption of Li^+ ions from a LiCl target of natural isotopic abundance. For ^6Li a preference of $27 \pm 3\%$ was determined relative to the natural isotope ratio of ^6Li and ^7Li.

3.4. Energy and Mass Correlations

The assumption of purely statistical ion desorption implies, that also at multiple desorption the ions emerge from different and independent locations around the track of the fission fragment. Studying yield of single mass lines in the Thiamine spectrum, however, a strong dependence between three positive ions was found. For instance, the relative intensity of the parent-like ion $M = 265$ increases distinctly as soon as the $M = 144$ mass line is suppressed. The regarded part of the Thiamine spectrum is presented in Figure 9.

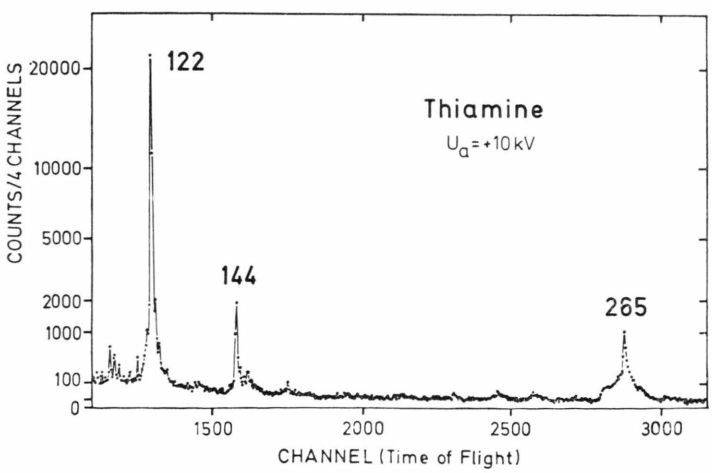

Fig. 9. Part of the Thiamine mass spectrum measured for positive ions at a flight distance of 120 cm.

In order to determine the correlation coefficient between two ions of mass A and B $(A<B)$ two spectra have to be taken, the first one starting with the line A, the second one with the line B. The measured intensities per fission fragment of the two mass lines are given by

1. spectrum $\begin{cases} I_1(A) = \varepsilon \cdot S(A) \,, \\ I_1(B) = \varepsilon \cdot S(B) - \alpha_{AB}\, \varepsilon^2 \cdot S(A)\, S(B) \,, \end{cases}$

2. spectrum $\{ I_2(B) = \varepsilon \cdot S(B) \,.$

Here $S(A)$ and $S(B)$ are the absolute yields per fission fragment and ε the overall detection efficiency at full acceptance. The correlation coefficient q is related to the parameter α_{AB} in the following way:

for correlations:

$q = (1-\alpha_{AB})/[1 - S(A)^{-1}]\,; \qquad 0 \leqq q \leqq 1 \,,$

for anticorrelations: $q = \alpha_{AB^{-1}}\,; \qquad 0 \geqq q \geqq -1 \,.$

In the case of Thiamine correlations and anticorrelations were observed for the molecular fragments $M = 122$ and 144 and the parent like ion $M = 265$. The coefficients are

$$q\,(122{,}144) = -\,(0.5 \pm 0.3)$$
$$q\,(122{,}265) = -\,(0.5 \pm 0.5)$$
$$q\,(144{,}265) = +\,(0.9 \pm 0.3) \,.$$

Three particle correlations have been neglected. This kind of correlations can be called "mass correlations". With help of coincidence methods [7] also first indications for "energy correlations" have been identified. Instead of starting the time-of-flight measurement with the fission fragment signal one can use the H^+-signal in the stop-detector as start event – gated by the fission fragment signal. If the velocity distributions of the proton and the considered ion are statistically independent, the mass line of this ion measured in coincidence to the protons should be the convolution of both single lines. In contrast to that the measurements show that the lines become more narrow.

The correlations of the Thiamine ions have to be the result of reactions between molecules or molecule ions at the surface. If the correlation coefficients are large, most of the simultaneously emitted ions belong to the same reaction process, i. e. to the same molecule cluster. Measuring correlations by this technique should open a new way to study the dynamics of ion-molecular reactions. We hesitate to examine the method for the analysis of chemical mixtures.

4. Discussion

Analizing the measured initial energy distributions in terms of a direct evaporation process would lead to the conclusion that the ions are emitted from regions of extremely high temperatures. In the case of $^{133}Cs^+$ these temperatures would not be as high as surmised in Ref. [4], but nevertheless 25 000 °C. As recently found by Comsa et al.[12], however, the mean energy of molecules evaporating from hot surfaces matches to temperatures distinctly higher than the actual surface temperature. Besides other explanations [13] one reason for this phenomenon could be the stochastical distribution of the surface potential, especially present in the case of contaminated targets. Such a potential distribution would act like a filter for low energetic ions, i. e. would hinder the emission of slow ions and shift the mean axial energy $\bar{E}_z$ to higher values. This effect was proved by Monte Carlo calculations with model surfaces assuming ion emission out of thermal equilibrium. Details of these calculations will be the subject of a future paper [14]. A preliminary result is that the measured energy distributions for Li, Cs and Atropine ions can be reproduced with an excitation temperature of about 3000 °C. It is worth mentioning that the calculations give always $1/\lambda_z > kT$.

Angular distributions evaluated also by this Monte Carlo method show a preference for ion emission into forward directions, again due to the stochastical potential distribution. If the radial and axial energy distributions are assumed to be independent of each other, they can be used to determine the angular distribution. For $^{133}Cs^+$ ions this semi-experimental result is

$$\Delta N/\Delta\Omega \sim \cos^n \Theta \quad \text{with} \quad n = 2.5 \pm 1 \,.$$

Other effects like field emission, recapture from antibonding states or by tunnelling [15] would cause also forward directed ion emission, but they are probably not responsible in this case.

A particular behaviour was found for the positive hydrogen ions. According to the initial energy distribution the H^+ ions seem to be much hotter than heavier ions and also the H^- ions [10]. Their angular distribution is forward directed like $\cos^5 \Theta$. This might be due to the special binding conditions of H^+ at the surface and the fact that H^+ will be the more abundant the higher the excitation energy of the organic material is.

The pronounced isotopic effect in the case of the $^6Li/^7Li$ yield disagrees again strongly with thermal equilibrium processes at high temperatures. The preference of the lighter isotope ^6Li can be understood proposing oscillatory binding states at the surface combined with a stochastic potential distribution.

The amount of inner energy transferred to the molecules at the surface can be estimated comparing the fragmentation pattern of fission fragment induced desorption with mass spectra obtained by other methods. Our spectra show similarities to field desorption spectra taken with heated targets, but also to spectra of Veith [16] produced by field desorption using unactivated emitters. From this we deduce the inner energy transferred at fission fragment induced desorption to be only 0.15 to 0.2 eV. Recently also SIMS spectra have become available taken by Benninghoven and Sichtermann [17] on organic targets with 2.5 keV Argon ions. Comparing fragmentation pattern and molecular ion yields, there are several similarities.

The remaining question is what kind of mechanism is responsible for the desorption and the transfer of energy to inner degrees of freedom. Evaporation via a direct thermal contact to the plasma formed along the track of the fission fragment is not in agreement with most of the observations. Direct impact processes or statistically distributed impact cascades are known to be the reason for sputtering neutral or charged particles from the surface at low energy ion bombardement. In agreement with this desorption mechanism the spectra of Ref. [17] show strong lines of metal ions of the target carrier foil. In our spectra metal ions of the Al, Ni and Cu carrier foils never have been observed, that means, the contribution of atomic impact processes is very small.

It is interesting to note that in SIMS experiments performed by Benninghoven and Sichtermann the extremely heteropolar bounded ions are much less abundant than in our spectra. Little contaminations of Na or K lead to intensive Na^+ and K^+ lines. The fission fragment induced desorption process seems to affect particularly heteropolar bounded species.

Fast heavy ions such as fission fragments loose their energy mainly by production of secondary electrons [18]. Without doubt either these secondary electrons or the direct strong Coulomb interaction are able to excite the electron plasma of the solid state system. Our hypothesis is that this excitation of the electron plasma causes a strong high frequency perturbation of Coulomb fields at the surface affecting especially polar binding states. This process would transfer energy to the inner degrees of freedom of the molecules too, causing fragmentation and elimination reactions. The energy transfer would be sufficient to liberate molecules also from weak Van-der-Waals bonds with certain probability. Special properties of the electron plasma excitation have to be considered in detail as, for instance, their frequencies and amplitudes entering the transition rates. These calculations will be handled in a future paper [14]. Up to now the experimental results are not in disagreement with this hypothesis. It can not be excluded that small additional surface charges are able to enhance the desorption. The energy gain by this effect, however, would be less than $E_0 = 1$ eV (see Chapter 3.2).

5. Conclusion

The desorption process seems to be mainly a result of the high frequency perturbation of the Coulomb fields at the surface. Little energy is transferred to vibration and rotation modes of the molecules leading to moderate temperatures and solving Van-der-Waals bonds rather than organic bonds via exchange interaction. Due to the collective type of this interaction ionization by electron abstraction is very unlikely compared with ionization by ion(proton)-molecule reactions. The main result is the desorption of polar bounded substances without much internal excitation forming quasimolecular ions with fair intensity. However, the quantity of excitation energy is higher than in static field desorption causing fragmentation and elimination reactions. According to this paper, combining fission fragment induced desorption with the time-of-flight technique offers a variety of methods for mass spectroscopy. Non-volatile substances can be studied in the nanogramme region, but also molecular reactions at surfaces or the change of molecular energy states in contact to the surface are in the scope of these methods. We hope that experiments with better defined surface states available in an ultra high vacuum system will give the possibility to study surface reaction dynamics in more detail.

[1] R. D. Macfarlane, R. P. Skowronski, and D. F. Torgerson, Biochem. and Biophys. Res. Com. **60,** (2) 616 [1974].
[2] O. Becker, N. Fürstenau, W. Knippelberg, and F. R. Krueger, Organic Mass Spectroscopy, in press.
[3] C. J. McNeal and R. D. Macfarlane, ACS National Meeting, Chicago, Illinois, August 1975, reprint.
[4] R. D. Macfarlane and D. F. Torgerson, Phys. Rev. Lett. **36,** 486 [1976].
[5] R. D. Macfarlane and D. F. Torgerson, Int. J. of Mass Spectr. and Ion Phys. **21,** 81 [1976].
[6] R. D. Macfarlane and D. F. Torgerson, Science **191,** 920 [1976].
[7] O. Becker, N. Fürstenau, F. R. Krueger, G. Weiß, and K. Wien, Nucl. Instr. Meth. **139,** 195 [1976].
[8] N. Fürstenau and W. Knippelberg, Diploma thesis at the Institut für Kernphysik, Technische Hochschule Darmstadt 1977.
[9] E. Bruminx and G. Rudstam, Nucl. Instr. Meth. **13,** 131 [1961].
[10] R. D. Macfarlane and K. Wien, to be published.
[11] L. D. Owen, D. E. Salomon, R. S. Florek, and N. C. Thomas, A New Plateau in Channeltron Electron Multiplier Arrays-Characteristics, Bendix Corp., Ann Arbor, Michigan, 1971.
[12] G. Gomsa, R. David, and K. D. Rendulic, Phys. Rev. Letters **38,** 775 [1977].
[13] W. Van Willigen, Phys. Rev. Lett. **28 A,** 80 [1968].
[14] F. R. Krueger, in preparation.
[15] D. Menzel, in Interactions on Metal Surfaces, R. Gomer ed., Topics in Appl. Phys. Vol. 4, p. 101.
[16] A. Veith, Techn. Hochschule Darmstadt, private communication.
[17] A. Benninghoven and W. Sichtermann, Proc. 7th Int. Mass Spectr. Conf. Florence 1976 (in press) and to be published in Analytical Chemistry.
[18] K. E. Pferdekämper and H.-G. Clerc, Z. Physik **A 280,** 155 [1977].